Geomorphology 396 (2022) 108000

Contents lists available at ScienceDirect

Geomorphology

journal homepage: www.elsevier.com/locate/geomorph

Improving regional flood risk assessment using flood frequency and dendrogeomorphic analyses in mountain catchments impacted by tropical cyclones

Adolfo Quesada-Román [a,b,*], Juan Antonio Ballesteros-Cánovas [a,c], Sebastián Granados-Bolaños [b], Christian Birkel [b], Markus Stoffel [a,c,d]

[a] Climatic Change and Climate Impacts, Institute for Environmental Sciences, University of Geneva, Boulevard Carl-Vogt 66, CH-1205 Geneva, Switzerland
[b] Department of Geography and Water and Global Change Observatory, University of Costa Rica, 2060 San José, Costa Rica
[c] Dendrolab.ch, Department of Earth Sciences, University of Geneva, Boulevard Carl-Vogt 66, CH-1205 Geneva, Switzerland
[d] Department F.-A. Forel for Environmental and Aquatic Sciences, University of Geneva, Geneva, Switzerland

ARTICLE INFO

Article history:
Received 13 July 2021
Received in revised form 28 September 2021
Accepted 12 October 2021
Available online 23 October 2021

Keywords:
Disaster risk reduction
Dendrogeomorphology
Bayesian MCMC
UAV
Tropics
Térraba River
Costa Rica

ABSTRACT

River floods frequently occur when tropical cyclones hit land. Nonetheless, systematic, long-term discharge data remain rather scarce in many tropical countries, which prevent proper analysis of peak discharges occurring during floods. The Térraba catchment is the biggest and most dynamic catchment in Costa Rica. In this study, we developed regional flood-frequency analyses combining tree-ring based estimation and measurement of peak discharge at monitoring stations during tropical cyclones to derive flood quartiles. Flood quartiles were combined with the Topographic Wetness Index (TWI) to determine regional flood hazards along floodplains. The flood risk assessment was based on a high-resolution mapping of infrastructure, population density (as a measure of exposure), and a social development index (to represent vulnerability). We show that peak discharge of cyclone-induced floods can be assessed accurately with flood-frequency analyses including dendrogeomorphic reconstructions and systematic discharge measurements. We also show that regional flood risk assessments can be performed in large-scale catchments if both coarse and detailed inputs are used. The results of this study will be useful for the development of flood risk schemes promoting resilience of local populations.

1. Introduction

Tropical regions have faced substantial land-use changes, especially over the course of the twentieth century. These changes have increased vulnerability of settlements to severe weather-related hazards (Lawrence and Vandecar, 2015; Carabella et al., 2020) as they increase sediment yields and riverscape variations (Wohl, 2006; Piacentini et al., 2020). The problem is particularly acute in regions where tropical cyclones commonly occur, resulting in intense floods with widespread, negative socio-economic consequences for local populations (Syvitski et al., 2014; Rodríguez-Morata et al., 2018). Tropical cyclones have repeatedly provoked intense devastation, and damage has often been aggravated by widespread urbanization and the lack of flood hazard assessments (Raymond et al., 2020).

Furthermore, proper flood hazard assessments depend on reliable data on the spatiotemporal distribution of rainfall events and discharge along rivers (Baker, 2008; IPCC, 2014; UNDRR – United Nations Disaster Risk Reduction, 2019; Guerriero et al., 2020). In tropical countries, this information is commonly limited or of poor quality, which in turn renders flood forecasts even more difficult (Wohl et al., 2012). In data-limited regions, different techniques can be applied to adequately estimate peak discharges and return periods of floods (Baker, 2008; Bodoque et al., 2015; Wilhelm et al., 2019; Bodoque et al., 2020).

Flood marks left in rivers can be used to determine spatial patterns and magnitudes of floods even months after an event (Borga et al., 2008). Botanical indicators provide relevant information to analyze, and date floods a posteriori to determine their magnitude (Ballesteros-Cánovas et al., 2015a). Botanical evidence of previous floods comprises injured stems and branches, tilted trunks, and exposed roots of trees growing alongside fluvial reaches (Ballesteros-Cánovas et al., 2020a, 2020b; Bodoque et al., 2020; Stoffel et al., 2012). In addition, scars in trees can be used as paleostage indicators (PSI) that can be accurately dated (Ballesteros-Cánovas et al., 2011a, 2011b), thereby allowing the extension of flood records back in time

* Corresponding author at: Department of Geography and Water and Global Change Observatory, University of Costa Rica, 2060 San José, Costa Rica.
E-mail address: adolfo.quesada@gmail.com (A. Quesada-Román).

https://doi.org/10.1016/j.geomorph.2021.108000

(Ballesteros-Cánovas et al., 2015b) and to derive flood hazard zonation (Ballesteros-Cánovas et al., 2013; Brooks and George, 2015; Garrote et al., 2019; St. George et al., 2020).

For engineering projects and flood risk management (Nguyen et al., 2014; Díez-Herrero and Garrote, 2020), flood-frequency analyses are normally derived to define the relation between flood magnitude and the exceedance probability to assess the likelihood that a given flood discharge will occur in the future (Wilhelm et al., 2019). A suite of approaches can be used to decrease the uncertainties of in situ flood-frequency analyses to produce more accurate flood magnitude estimates based on larger sample sizes (Gaál et al., 2010). These approaches can extend these analyses spatially (e.g., Hosking and Wallis, 1997) and temporally by using information provided by paleofloods or historical floods (e.g., Reis and Stedinger, 2005). Bayesian Markov Chain Monte Carlo (MCMC) approaches provide a precise statistical tool to perform flood-frequency analyses (Gaume, 2018). In a context where flow records are limited or incomplete, historical evidence can help to reduce uncertainties in flood magnitude, even if they are not as accurate as direct measurements (Baker, 2008; Benito et al., 2015).

Risk management strategies primarily aim at reducing risks and losses (UNDRR – United Nations Disaster Risk Reduction, 2019). Flood risk management can be achieved by implementing legal, economic, political, educational, structural, technological, cultural, social, health, environmental, and institutional measures to reduce and prevent hazard, vulnerability, and exposure (IPCC, 2014; UNISDR, 2015). This involves a holistic and comprehensive understanding of hazards at the local level, including flood risk (Pinto Santos et al., 2020). Like discharge data, tropical regions also lack information on economic losses caused by floods, which limits the potential to perform risk analyses (de Ruiter et al., 2020).

In Costa Rica, more than 90% of disasters are hydrometeorological (LA RED, 2018). Therefore, work on flood processes has been extensive in Costa Rica; whereas the resolution of hazard maps that combine information on exposure, vulnerability, and risk has remained largely unexplored (Quesada-Román and Mata-Cambronero, 2020). In the Térraba catchment, where this study was conducted, the ongoing changes in land cover from forests to extensive croplands have substantially intensified rates of erosion and sediment yield (Krishnaswamy et al., 2001b). As a result, intense floods now occur in the Térraba catchment during the passage of tropical cyclones, at roughly decadal intervals (Quesada-Román and Zamorano-Orozco, 2019a). Floods affect different parts of the catchment where they claim lives and cause damage to agriculture and communication infrastructure, particularly roads and bridges. Recent major hurricanes that led to severe floods in the Térraba catchment were Joan (1988) and Cesar (1996), as well as tropical storms Alma (2008) and Nate (2017) (Quesada-Román et al., 2020b). These tropical cyclones claimed dozens of lives, affected the property of hundreds of people, and caused substantial economic losses (Table 1). A clear need exists to adapt to strong tropical rainfall events (including, but not restricted to tropical cyclones) because these events are expected to become more frequent as climate warming continues (Saunders and Lea, 2008). In this perspective, the creation of a regional flood-frequency analysis and a risk assessment could help land-use planning and disaster risk reduction. This paper, therefore, aims at (i) developing a regional flood-frequency analysis employing dendrogeomorphic records, and (ii) providing a risk assessment of floods occurring during tropical cyclones in the Térraba catchment (Costa Rica).

2. Materials and methods

Fig. 1 presents an overview of the approaches used in this study: (1) study site selection based on historical / flow gauge records, (2) acquisition of topographic and geomorphic data, (3) tree-ring based flood reconstruction, (4) hydraulic and statistical modeling, and (5) flood risk assessment based on exposure and vulnerability data.

2.1. Geographic setting

The Térraba catchment (4765 km^2) is in the southeast of Costa Rica from 8.7° to 9.5° N and 82.7° to 83.8° W (Fig. 2). The Térraba catchment and its sub-catchments have a strong tectonic control by local faults with a NE-SW and NW-SE alignment. Lithology is composed both of Mio-Pliocene (volcanic) and Oligocene-Miocene (sedimentary) rocks with very regular grain sizes among boulders and coarse sands in all sub-catchments (Denyer and Alvarado, 2007; Alvarado et al., 2017; Gardner et al., 2013). The Mio-Pliocene volcanic rocks are impermeable intrusive stocks and batholiths composed mostly of gabbros and extrusive volcanic rocks such as andesitic-basaltic rocks formed by lavas with prismatic fractures. These volcanic intrusive rocks rest beneath the Oligocene-Miocene sedimentary rocks, comprising permeable breccias, sandstones, and shales with textures from decimeters to meters.

The highest peak in the country, Cerro Chirripó (3820 m asl), marks the origin of the headwaters (Veas-Ayala et al., 2018; Quesada-Román et al., 2019, 2020c, 2021) from where it crosses the General-Coto Brus Valley and the Térraba-Sierpe deltaic mangrove wetlands to flow into the Pacific Ocean (Acuña-Piedra and Quesada-Román, 2016, 2021; Quesada-Román and Zamorano-Orozco, 2019b). The postglacial alluvial fans and floodplains (Camacho et al., 2020) along the General-Coto Brus Valley are used currently for intense agriculture and former forests have been turned into croplands, especially after the 1950s – the same area is now affected by high erosion rates (Krishnaswamy et al., 2001a). The catchment outlet is in Palmar where the river becomes a delta covered mainly by mangrove. Roughly 256,000 people live in the Térraba catchment (in 2020), of which 143,000 inhabitants live in Pérez Zeledón, followed by Buenos Aires (53,000 inhabitants), Coto Brus (44,000), and Osa (16,000). The municipalities of Buenos Aires and Coto Brus are also the home of roughly 30% and 10% of indigenous people, respectively (INEC - Instituto Nacional de Estadística y Censos, 2020).

2.2. Climate characteristics and tropical cyclones

Local climate is dominated by the movement of the Intertropical Convergence Zone, cold fronts, the northeast trade winds, the Atlantic Multidecadal Oscillations (AMO), the El Niño-Southern Oscillation (ENSO), and the seasonal influence of tropical cyclones originating in the Caribbean (Hidalgo et al., 2015; Durán-Quesada et al., 2020; Quesada-Román et al., 2020a). This setting results in two rainfall maxima producing between 1500 (lowlands and confluences) and 6000 mm (mountain tributaries) annually, the first one in May and the second one in October. These maxima are disconnected from each other by the Midsummer Drought, which lasts from July to August (Maldonado et al., 2016). The dry season extends from December to April. Annual mean temperatures range from 8 to 28 °C, mostly depending on altitude (IMN - Instituto Meteorológico Nacional, 2008). Floods are triggered by strong local convection, but intense floods are normally related to the passage of tropical cyclones (Durán-Quesada et al., 2020). Devastating tropical cyclones over the Térraba River catchment occur every ten years on average (Table 1).

2.3. Reconstruction of recent flood event

We chose seven sampling sites along the Térraba catchment to determine the peak discharge reconstruction employing botanical evidence, in particular scars in trees (see Quesada-Román et al., 2020b for methodological details). In the field, during January of both 2018 and 2019, we sampled trees with flood scars that could be clearly attributed to Tropical Storm Nate in 2017 (Sigafoos, 1964; Ballesteros-Cánovas et al., 2011a). The position of scarred trees was documented with a Global Positioning System (GPS; accuracy of <1 m) and scar heights were measured from the base of the tree to the central height of the injury (Ballesteros-Cánovas et al., 2011b, 2015a, b). The two-dimensional (2D) hydrodynamic model IBER (www.iberaula.es) was

Table 1
Tropical cyclones that affected the Térraba catchment between 1970 and 2018 (LA RED, 2018).

Date	Municipalities affected	Tropical cyclone	Impacts
9/19/1971	Pérez Zeledón, Osa	Tropical Storm Irene	1 death, 18 victims, 1 home destroyed and 8 affected
10/22/1988	Osa	Hurricane Joan	1200 victims
7/25/1996	Pérez Zeledón, Buenos Aires, Osa	Hurricane Cesar	13 deaths, thousands of victims, 449 houses destroyed
10/22/1998	Pérez Zeledón, Buenos Aires, Coto Brus, Osa	Hurricane Mitch	954 victims, 18 houses destroyed, 592 houses affected
5/29/2008	Pérez Zeledón, Buenos Aires, Osa	Tropical Storm Alma	900 affected
10/5/2017	Pérez Zeledón, Buenos Aires, Coto Brus, Osa	Tropical Storm Nate	640 victims, 160 houses affected, $15 US million in economic losses

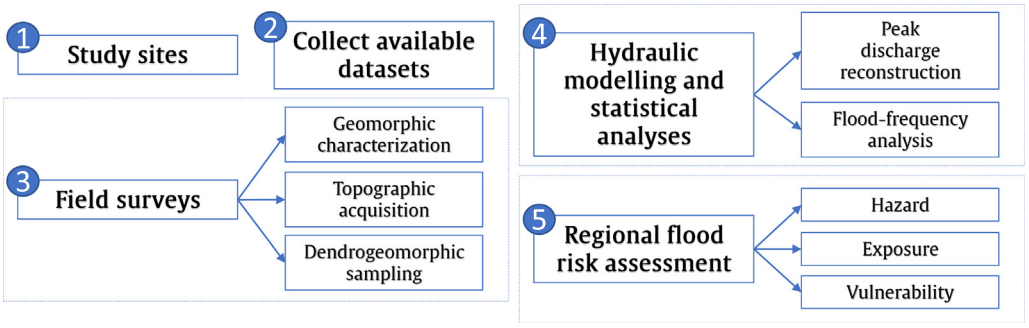

Fig. 1. Conceptual diagram summarizing the regional flood-frequency analysis approach employed at the Térraba catchment.

employed to model water depth for the flood of 2017 in all the sampling sites of the Térraba catchment (see Fig. 1 for details).

IBER replicates unsteady surface flows, turbulent-free, and environmental processes in riverscapes by resolving depth-averaged 2D shallow water equations (2D Saint-Venant) using a finite volume approach with a second-order roe arrangement (Cea et al., 2019). The model is suitable for turbulent mountain streams where discontinuities are common. Even in intermittent regimes, the method is conservative.

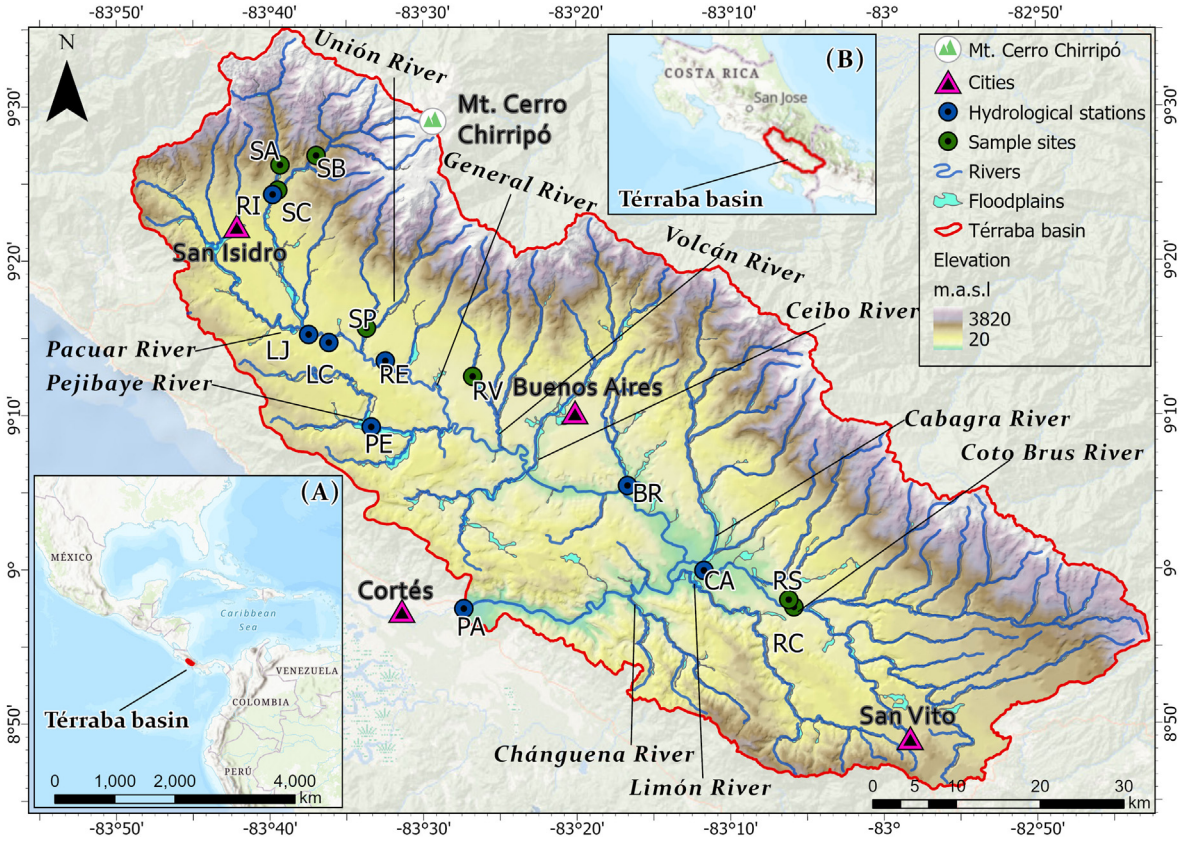

Fig. 2. Location of the Térraba catchment in Central America (A) and within Costa Rica (B). Tree-ring sampling sites are shown with green dots, hydrological stations with blue dots. For acronyms see Table 2. (For interpretation of the references to colour in this figure legend, the reader is referred to the web version of this article.)

The model operates in a non-structured mesh comprising triangles or quadrilateral features. We used an Unmanned Aerial Vehicule (UAV; DJI Phantom 4 Pro V2) to acquire digital imagery. Using a Structure from Motion (SfM) approach we geo-rectified ortho-mosaics and obtained digital elevation models (Turner et al., 2012). Agisoft Photoscan 1.4.0 was used to reconstruct riverscapes and to produce elevation models with a 0.5 m resolution (Langhammer and Vacková, 2018).

SfM derived from aerial digital imagery can produce both digital surface models and bare terrain models if the densified point cloud is classified into different categories to interpolate only the desired data, which in this case was terrain and channel characteristics. These data can be used for hydraulic modeling of floods and stream behavior as shown by Quesada-Román (2020, 2021) and Langhammer and Vacková (2018). We are aware that aerial digital imagery cannot perform bathymetric analysis of water bodies. Unfortunately, during the research, we did not have LIDAR or bathymetric equipment that allowed us to perform accurate measurements of the riverbed. Nevertheless, we consider the data on channel characteristics obtained by the UAV to be adequate for the hydraulic modeling of floods. UAV surveying is a robust tool to obtain channel data and geometry for hydraulic modeling and fluvial geomorphology purposes (Granados-Bolaños et al., 2021; Vélez-Nicolás et al., 2021).

We used Manning's n roughness coefficient for homogenous roughness units to evaluate bed friction in the field (Chow, 1959). For the main channel we used $n = 0.075$, 0.16 for forests and 0.08 for areas with sparse vegetation (Barnes, 1967; Arcement and Schneider, 1989). Consecutive input discharges (i.e., steady flow regime) were modeled based on historical extremes (applying steps from 100 to 1500 m^3/s). The 2017 flood peak discharge was modeled with an iterative step-backwater method, and it entailed an (i) estimate of water stages from modeled peak discharges, and (ii) a fitting of resulting modeled water surfaces with PSI heights recognized at the sampling sites (Webb and Jarrett, 2002). We then determined the mean squared error (MSE) of each modeled discharge against the height each scar. The magnitude of the flood in each river section was then characterized as the peak discharge for which the MSE between the model and the scar heights was smaller (Fig. S1; Quesada-Román et al., 2020b).

2.4. Regional flood-frequency analysis

Reconstructed peak discharge values and related uncertainty were included as a range of values to the systematic records of annual maximum discharge from eight hydrological stations from 1962 to 2019 (Table 2; Table S2; ICE - Instituto Costarricense de Electricidad, 2019). We then utilized the available data to implement a regional flood-frequency analysis using Bayesian Markov Monte Carlo Chain (MCMC) algorithm (Gaál et al., 2010; Gaume, 2018). Moreover, a Generalized Extreme Value distribution (GEV) was applied to calculate flood quantiles. Uniformity of the existing systematic flow series was verified using the Hosking and Wallis (1987) algorithm (Table S1), which highlights the difference among sites in samples Lcv (coefficient of L-variation) for the evaluated sectors (Fig. S2). A regional flood-frequency analysis thus permits the addition of flood quantile estimations at distinct catchment positions by flow-index regionalization (Figs. S3, S4). This approach is based on the distribution of a flow discharge from dissimilar catchments of a larger and single basin (Fig. S5). This analysis was completed using the R package nsRFA (Viglione, 2013). The strength of this method has been tested previously in other hydrological contexts (Reis and Stedinger, 2005; Gaume et al., 2010; Ballesteros-Cánovas et al., 2015b, 2016, 2017). Finally, we added historical peak discharges from Tropical Storm Nate 2017 obtained with the dendrogeomorphic approach as they are expected to improve flood quantiles and reduce uncertainties at each reach analyzed within the catchment (Fig. 3; Bodoque et al., 2020). We then calculated the occurrence of floods with different exceedance probabilities per catchment surface unit (1 km^2) (Table S3).

Table 2
Hydraulic model estimated peak discharge at sites 1–7 and observed peak flows at hydrological stations 8–15 used for the regional flood-frequency analysis in the Térraba catchment.

Number	Code	Name	Area (km^2)	Maximum peak discharge (m^3/s)	Year
1	SA	Site A (Pueblo Nuevo)	101	636	2017
2	SB	Site B (Canaán)	164	455	2017
3	SC	Site C (Miraflores)	206	1249	2017
4	SP	San Pedro	68	146	2017
5	RV	Río Volcán	66	143	2017
6	RC	Río Coto Brus	852	336	2017
7	RS	Río Sábalo	54	212	2017
8	RI	Rivas	317	947	2017
9	LJ	Las Juntas	823	2007	2005
10	LC	La Cuesta	843	2776	2017
11	RE	Remolino	1071	5250	1996
12	PE	Pejibaye	129	1373	1993
13	BR	El Brujo	2399	8809	1996
14	CA	Caracucho	1135	3366	1996
15	PA	Palmar	4766	13,500	1996

2.5. Regional flood risk assessment

To identify flood-prone areas within the Térraba catchment and subsequently define the flood hazard, we performed a hydrogeomorphic floodplain mapping (GFPLAIN) using the algorithm developed by Nardi et al. (2008, 2019) and parameters provided by the 10-m DEM following Annis et al. (2019). To separate differences in flood hazard within the identified floodplains, we used the Topographic Wetness Index (TWI) because it merges local upslope contributing area and slope, i.e., variables frequently applied to quantify topographic control in hydrological processes (Sörensen et al., 2006). Moreover, the TWI was multiplied by the flood magnitude for a return period $T = 10$ yr (Table S3), which corresponds, on average, to the frequency of historical observations of tropical storms affecting the catchment. The exposure to floods was defined with the population density and infrastructure product of WorldPop (Tatem, 2017) as it provides the best resolved estimate based on machine learning approaches for the number of people residing in 100 × 100 m grid cells. For the assessment of flood vulnerability, we utilized the social development index (MIDEPLAN - Ministerio de Planificación Nacional y Política Económica, 2017) developed by the Costa Rican Ministry of National Planning and Economic Policy (MIDEPLAN). This index gathers and evaluates educational, security, economic, public health, and civic participation variables for all districts of the Térraba catchment (MIDEPLAN - Ministerio de Planificación Nacional y Política Económica, 2017). All variables were normalized from 0 to 1 (Fig. S5).

Flood risk gives the likelihood for the occurrence of a flood that has the potential to produce impacts to infrastructure, people, and property (Pinto Santos et al., 2020). The risk of flooding at the catchment level implies a direct probabilistic relation between the physical processes of flooding and given exposed and vulnerable elements (Pinto Santos et al., 2019). Flood risk (FR) is thus a dimensionless and equivalent calculation at the catchment level and is the result of hazard (H), exposure (E), and vulnerability (V):

$$FR = H^{\frac{1}{3}} * E^{\frac{1}{3}} * V^{\frac{1}{3}} \quad (1)$$

This expression of flood risk considering the scale, risk components, and input data differences is based on the INFORM risk index (De Groeve et al., 2014). When compared to the simple product of H, E, and V, used without the exponentiation, one can observe a dispersal and increase in the range of final flood risk scores. Finally, we produced a point map with the flood risk categorized as high, medium, and low using Jenks natural breaks classification method for practical applications (Jiang, 2013; Allen et al., 2018). In our analysis, because of the limited information available, we did not include and/or value economic losses.

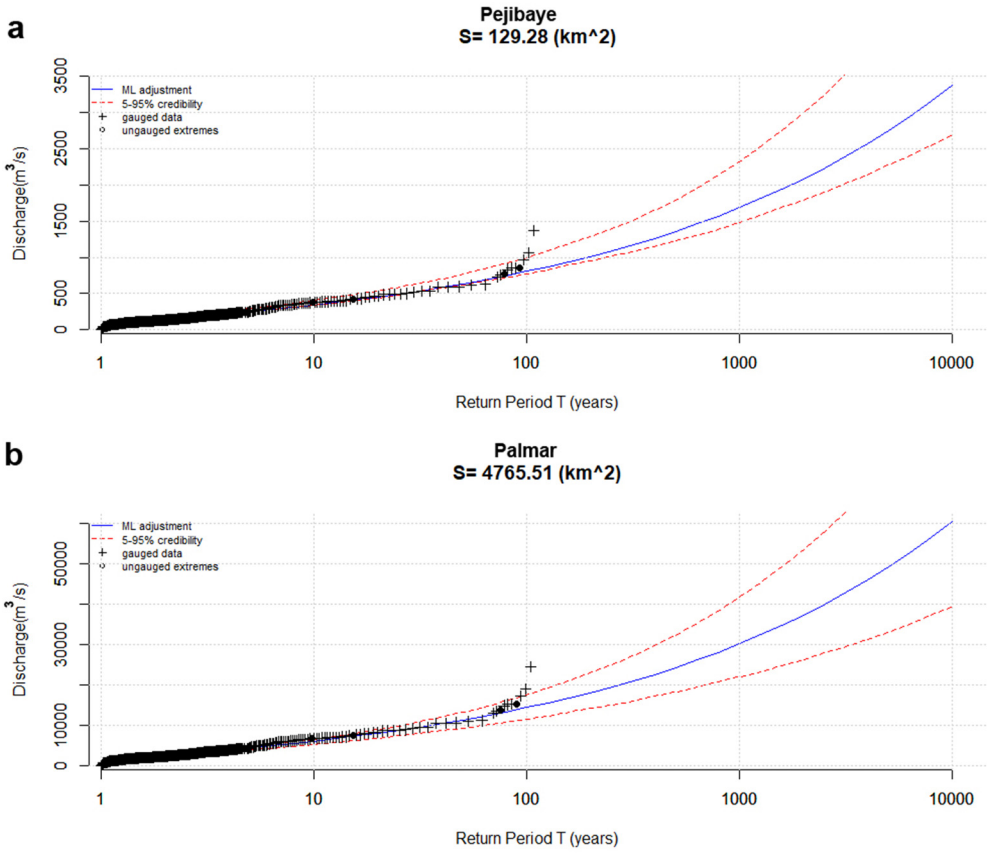

Fig. 3. Flood frequency distribution derived from systematic flow-gauge series and the reconstructed paleodischarges at the level of the gauge stations with the smallest (a) and the largest (b) drainage areas in the Térraba catchment.

3. Results

3.1. Discharge reconstruction of a flood triggered by Tropical storm Nate

We analyzed scars on 148 trees impacted by sediment and wood carried during the flood generated by Tropical Storm Nate (Table 3). The mean scar height in these trees was 1.74 m with an average standard deviation of 0.63 m. We found the highest scar heights at Site B with an average of 2.57 ± 0.73 m over the channel bed whereas the lowest scar heights were found in San Pedro with an average of 1.03 ± 0.66 m. The average of the estimated mean square error (MSE) between observed scar heights and simulated water depths was 1.39 m for all the sampling sites. The hydraulic model indicates that discharge at the seven sites during the 2017 flood ranged from 143 to 1249 m^3/s (Table 2).

3.2. Ungauged floods and regional flood-frequency analysis

We applied the Hosking and Wallis test to eight flow gauge records (1962–2019) covering catchment areas ranging from 129 to 4765 km^2. The test yielded a H1 value of −0.40, showing that the dataset used in this study can be assumed homogeneous (i.e., H1 ≤ 1; see Supplementary Information; Table S1). Based on the eight available flow gauge records and the seven modeled (historical) peak discharges, we identified the resulting flood frequency for a runoff surface of 1 km^2 during which a flow surpassed the 90th percentile for the record length (Table S3). Fig. 3 provides an example of the fit of the distribution function with uncertainties at the 90% confidence level, amid the obtained regional flood frequencies and extrapolated estimates based on flow gauge data from the Pejibaye and Palmar stations. All station records are provided in Table S2. Inclusion of the reconstructed flood discharges suggests that the flood hazard has been underestimated by <10.7% using systematic records alone and uncertainties ranging between the 5th and 95th percentiles (Table 4). Large uncertainties (56.2% and 80.3%) are found in smaller catchments RI (317 km^2) and LJ (823 km^2) where local faults are found with a NE-SW orientation at RI, and a tectonic depression axis along the valley bottom at LJ. In the larger sub-catchments uncertainties are much smaller (e.g., <12.6% at PA). Variability in the uncertainties is presumably related to differences in catchment area between the different stations. Other key factors are their orientation (with RI, CA, and PA having a NE–SW, and LJ, LC, RE, PE, and BR a NW–SE bearing), tectonic control by regional or local faults, as well as differences in lithology (RI and CA mostly have volcanic substrates, PE is a sedimentary catchment while the rest are composed of both volcanic and sedimentary bedrock). Stations with large (BR and PA) and small (RI, PE, and LJ) catchment areas produced intermediate and higher differences between observed (i.e., measured) and reconstructed values, respectively. In contrast, the stations of intermediate size (RE, LC, and CA) had the smallest uncertainties between systematic and nonsystematic records.

3.3. Flood risk assessment

To adequately represent flood hazard (H), we determined the hydrogeomorphic floodplain of the Térraba catchment and combined the 10-yr return period with the TWI. Using the spatial distribution of the hazard as obtained with the Jenks natural breaks classification method, we obtained a graded differentiation between the northern and western sub-catchments (i.e., General, Pacuar, Unión, Volcán, and Ceibo) where low and medium flood hazards are found, and high and moderate flood

Table 3
Dendrogeomorphic attributes of the trees used as paleostage indicators (PSI) for each study reach.

Study reach	Number of scars in trees	Mean scar height (m)	MSE	Drainage area (km^2)	Calculated peak discharge (m^3/s)
Site A (Pueblo Nuevo)	29	2.25 ± 0.70	1.46	101	636
Site B (Canaán)	31	2.57 ± 0.73	1.64	164	455
Site C (Miraflores)	31	2.15 ± 0.78	2.1	206	1249
San Pedro	15	1.03 ± 0.66	1.05	68	146
Río Volcán	9	1.63 ± 0.38	0.88	66	143
Río Coto Brus	17	1.10 ± 0.47	1.13	851	336
Río Sábalo	16	1.46 ± 0.70	1.49	54	212

Table 4
Comparison of flood magnitude for the 10 yr return period estimates in the Térraba catchment before and after inclusion of the reconstructed peak discharges. ML – mean values, X5, X95–5% and 95% uncertainties, respectively.

Code	Drainage area (km^2)	ONLY SYST RI = 10 yr			SYST + NONSYST RI = 10 yr			OBSERVED CHANGES (%)		
		ML	X5	X95	ML	X5	X95	ML	X5	X95
RI	317	393	340	537	710	709	886	80.3	−98.9	−31.9
LJ	823	970	837	1252	1516	1450	1750	56.2	−68.4	−46.9
LC	842	1534	1285	2057	1566	1457	1751	2.1	−56.9	−65.4
RE	1070	1915	1501	2715	1899	1731	2099	−0.87	−59.2	−74.7
PE	129	714	535	1372	358	341	446	−49.8	−80.3	−73.5
BR	2399	3899	3417	4141	3527	3177	3885	−9.5	−19.6	63.2
CA	1134	2109	1759	2681	1993	1808	2189	−5.5	−44.4	−63.6
PA	4765	5491	4617	6121	6184	5266	6896	12.6	−6.6	0.13

hazards in the medium-sized, south, and southeast-oriented sub-catchments (including Pejibaye, Cabagra, Coto Brus, Limón, and Chánguena) (Fig. 4).

Exposure (E) behaves mostly in the opposite way when compared to flood hazard except in urban centers. In fact, the General, Pacuar, and Ceibo sub-catchments are influenced by important urban centers (such as San Isidro del General). In addition, urbanized surroundings are found to the northwest as well as at Buenos Aires at the center of the Térraba catchment (Fig. 5). These areas therefore exhibit intermediate to high exposure values because of their high population and

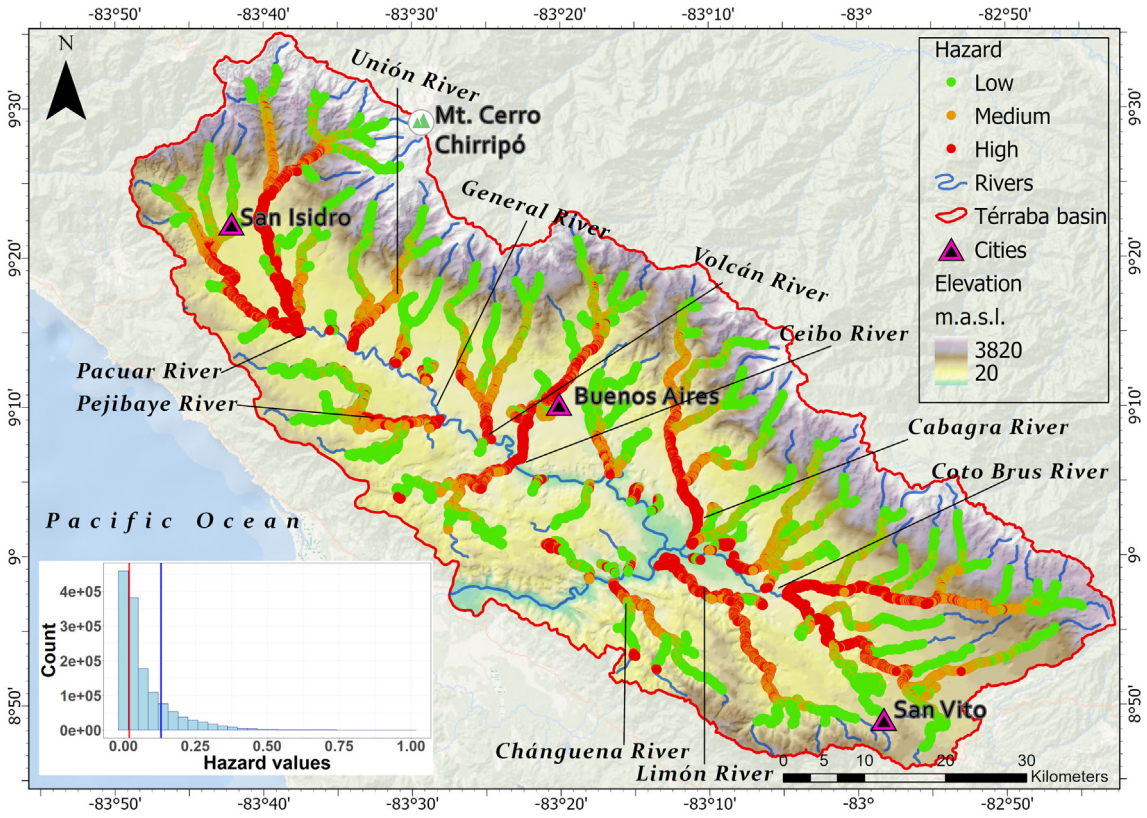

Fig. 4. Flood hazard map of the Térraba catchment, Costa Rica. The inset histogram shows the lower (red line) and upper (blue line) threshold values. (For interpretation of the references to colour in this figure legend, the reader is referred to the web version of this article.)

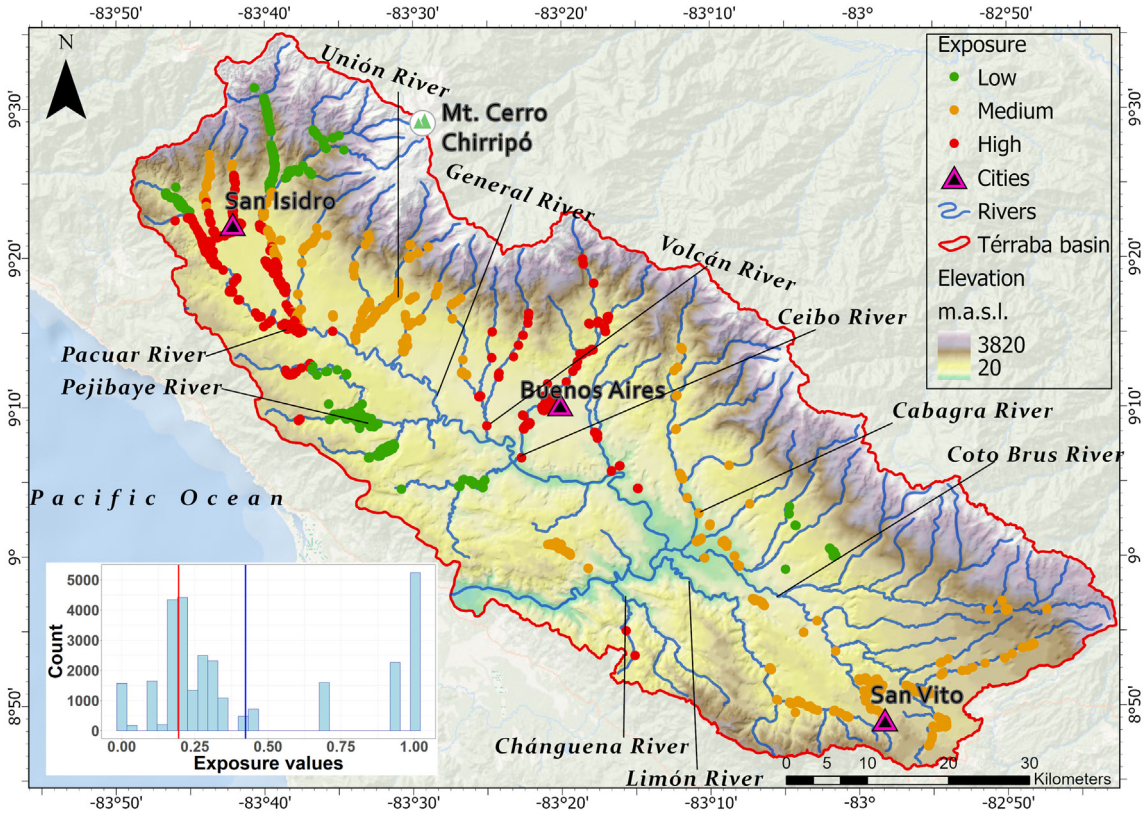

Fig. 5. Exposure map of the Térraba catchment, Costa Rica. The inset histogram shows the lower (red line) and upper (blue line) threshold values. (For interpretation of the references to colour in this figure legend, the reader is referred to the web version of this article.)

infrastructure density. The remainder of the catchment is primarily rural with very low population and infrastructure densities and thus produce low exposure values.

Spatial differences in vulnerability (V) follow a dissimilar pattern that the exposure with a graded differentiation between the northwestern to the south-southeast parts of the sub-catchments (Fig. 6). The major cities of San Isidro del General and San Vito have lower vulnerability values. Higher vulnerability values are, in contrast, strongly linked to rural areas with a majority of extensive or subsistence agricultural activities and the indigenous territories within the municipalities of Buenos Aires and Coto Brus.

In terms of risk (Fig. 7), the highest values can be localized in several areas along the Térraba catchment, sometimes in isolated spots, but mainly within the General, Unión, Pejibaye, Ceibo, and Limón subcatchments, where population densities are high, income is low, and/or found within indigenous territories. We obtained medium and low risk values especially in the least densely inhabited catchments with agricultural landscapes such as Pacuar, parts of General, Volcán, and Coto Brus. In total, approximately 6000 inhabitants are settled in the flood-prone areas of Térraba catchment.

4. Discussion

4.1. Flood-frequency analysis based on dendrogeomorphic reconstructions and hydraulic modeling

This study shows how peak discharge of a flood triggered by a tropical cyclone can be reconstructed retrospectively with a flood-frequency analysis using dendrogeomorphic reconstruction and flow gauge records. The information obtained can yield valuable information about past floods in an environment where data is scarce and new insights on flood frequency and magnitude can advise decision makers and residents. The flood frequency analysis carried out in several subcatchments of the Térraba catchment employed a classical approach that has been used widely for flood hazard cartography (Stephens and Bledsoe, 2020). Paleoflood and historical information can expand the record length and provide data extremes often missing in gauge records (Baker, 2008). Likewise, regional flood-frequency assessments have been used to combine nonsystematic and systematic records in a flow-index regionalization (Gaál et al., 2010; Gaume et al., 2010; Nguyen et al., 2014). In that sense, dendrochronology allows coupling of nonsystematic records with flow gauge records to reconstruct floods (Meko et al., 2012; Ballesteros-Cánovas et al., 2019).

The flood occurred during Tropical Storm Nate (Tables 1 and 2; ICE - Instituto Costarricense de Electricidad, 2019). Tropical cyclones provoke a regionalization of the rainfall distribution and often results in heterogeneous peak discharges. The complex hydrological regime of this tropical mountain catchment is enhanced by the energy and moisture available in the system, the high inter- and intra-annual variability (ENSO) of precipitation and the occurrence of high magnitude, yet infrequent extreme events (Krishnaswamy et al., 2001a). In addition, the catchment suffers from rainfall erosion caused by land uses that damages the soil and higher sediment delivery ratios with increasing catchment area (Krishnaswamy et al., 2001b; Krishnaswamy et al., 2018).

Our results are consistent with previous works: Ruiz-Villanueva et al. (2013) showed that uncertainty diminishes if historical information is included in small ungauged or poorly gauged mountain catchments. Ballesteros-Cánovas et al. (2013) demonstrated that nonsystematic data obtained from dendrogeomorphic approaches of riparian trees can be included in flood frequency analysis and integrated flood risk assessments. In the Tatra Mountains (Poland), Ballesteros-Cánovas et al. (2016) showed that the addition of non-systematic paleohydrological data derived from tree-ring series can have a critical impact on the resulting flood-frequency analysis. Ballesteros-Cánovas et al. (2017) also found in a study carried out in the Indian Himalaya

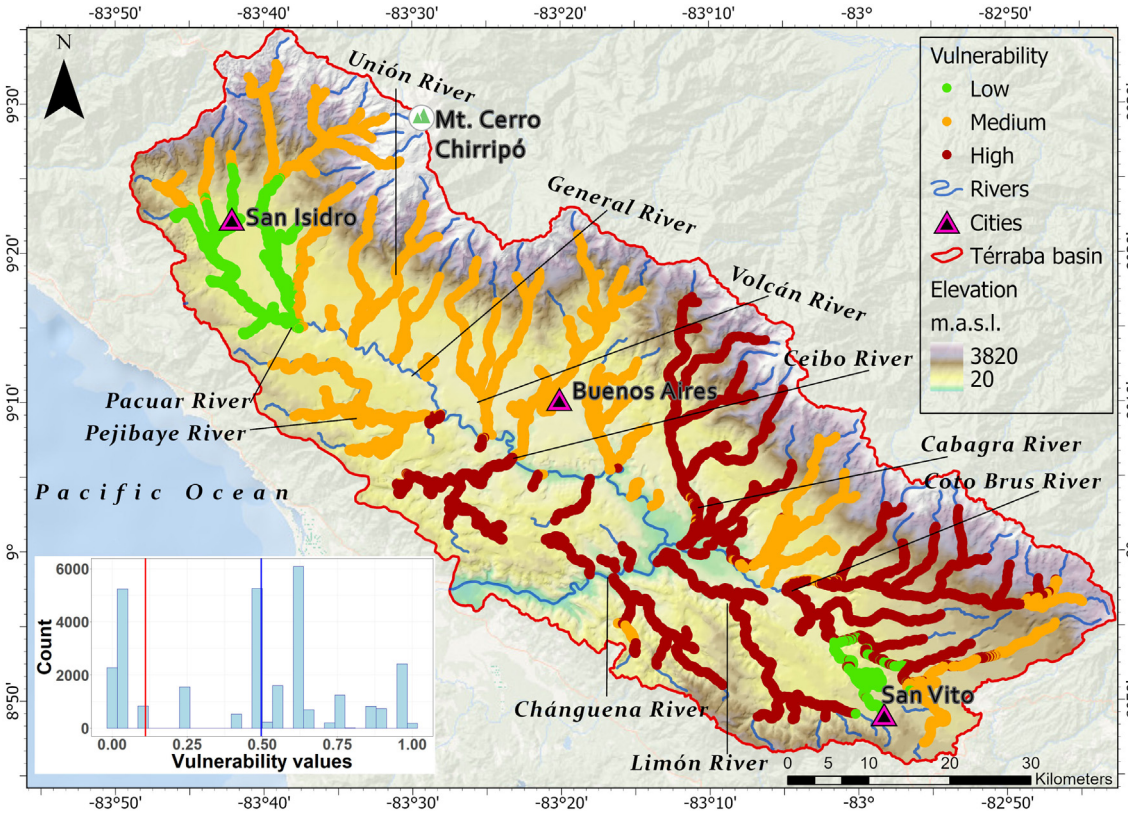

Fig. 6. Vulnerability map of the Térraba catchment, Costa Rica. The inset histogram shows the lower (red line) and upper (blue line) threshold values. (For interpretation of the references to colour in this figure legend, the reader is referred to the web version of this article.)

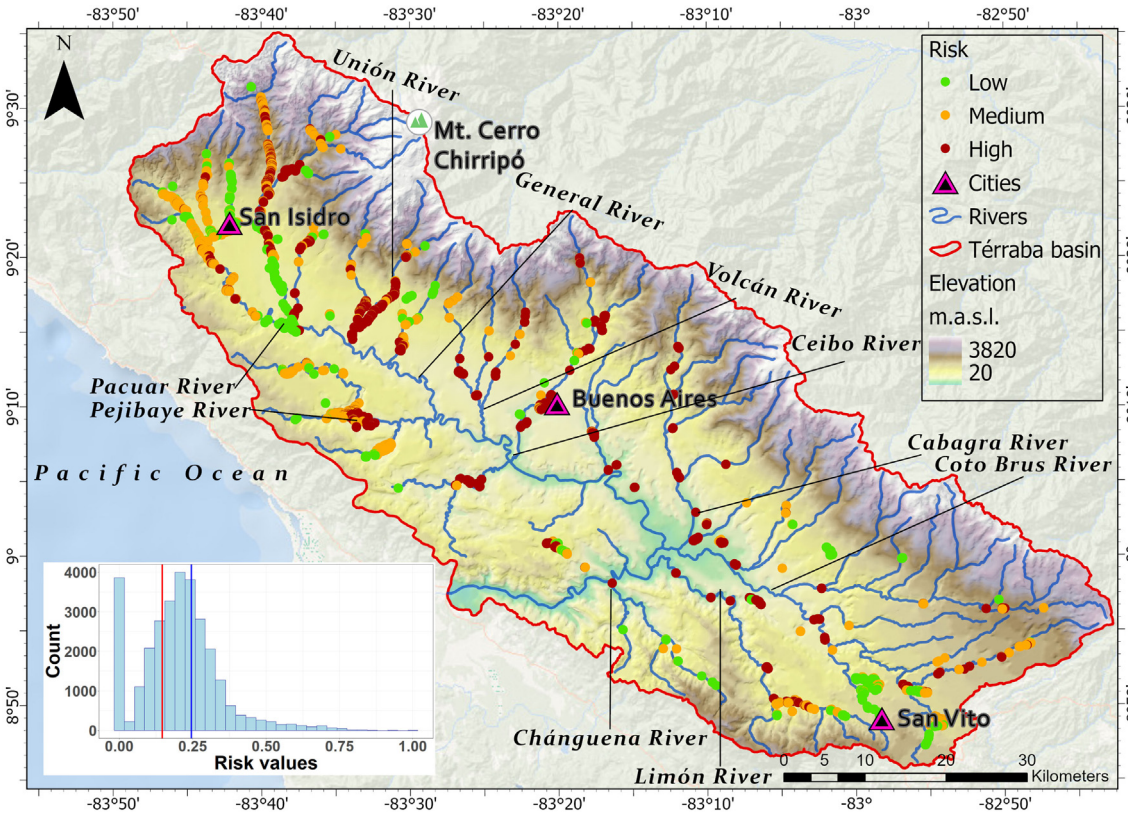

Fig. 7. Flood risk map of the Térraba catchment, Costa Rica. The inset histogram shows the lower (red line) and upper (blue line) threshold values. (For interpretation of the references to colour in this figure legend, the reader is referred to the web version of this article.)

that the insertion of non-systematic hydrological data from tree-ring series can have a significant influence on both the estimation of flood quantiles and uncertainties derived from flood-frequency analysis. In our study, we applied this approach and sampled trees in the vicinity of the Rivas, San Pedro, Sábalo, and Coto Brus gauging stations. Finally, flood hazard assessments at regional or large scales along the main river valleys prove useful to detect areas that are highly susceptible to future floods (Allen et al., 2018).

Limitations of regional flood-frequency assessments merging non-systematic and systematic records can be ascribed to the uncertainties in large catchments whose flow gauge data is less representative (Ruiz-Villanueva et al., 2013; Ballesteros-Cánovas et al., 2017). The uncertainties found are similar to those reported in previous studies (Quesada-Román et al., 2020b), especially in the lower sections of the Térraba catchment. Bigger sub-catchments (BR and PA) had intermediate observed changes, while small sub-catchments (RI, LJ and PE) showed the largest uncertainties. Mid-sized sub-catchments (LC, RE and CA) had lower uncertainties between systematic and non-systematic (dendrogeomorphic) records. The catchments with smaller uncertainties are normally larger in size and have clear tectonic or lithological controls. These results are consistent with a study that showed that tectonics, and not climate, exerted the dominant control on the shape of river longitudinal profiles globally and eventually in its uncertainties (Seybold et al., 2021).

We concentrated our analysis in the mountain headwater catchments, where systematic and non-systematic data was available, and reported peak discharges were consistent with our results (Quesada-Román, 2020). Although tree-rings have been used to improve flood risk, given the inherent difficulties to work in tropical environments, here such improvements are circumscribed to the characterization of the recent events, having a less relevant impact in the flood hazard assessment. We suggest the use of isotope analyses to distinguish the origin of tropical precipitation events and overcome with statistical assumptions in future studies (Sánchez-Murillo et al., 2019, 2020). We consider that the approach we employed can be implemented in other catchments that are commonly affected by tropical cyclones, phenomena which will become more intense and frequent in decades to come (Alvarado and Alfaro, 2003; Saunders and Lea, 2008; Walsh et al., 2016; Tennille and Ellis, 2017; Bhatia et al., 2019).

4.2. Improved regional flood risk assessment and potential applications

This study shows that regional flood risk assessments within large-scale geomorphic units – at scales of 10^3–10^4 km^2 (Dramis et al., 2011) – are feasible using an assemblage of coarse (hydrological stations data, social indexes) and detailed inputs (UAV data, hydraulic modeling, high-resolution population density spatio-temporal information). The hydrogeomorphic floodplains prove useful for the demarcation of flood-prone areas along the catchment, as previously reported by Annis et al. (2019) and Nardi et al. (2019). The combination of the hydrogeomorphic floodplains, TWI (Pourali et al., 2016), and the 10-yr return periods of floods during tropical cyclones allowed a regional flood hazard zonation. Whereas previous local studies have identified distinct flood hazard levels using geomorphic mapping techniques (Quesada-Román, 2016, 2017), most of them have associated tropical cyclones every 10 yr as the main triggers that relate to our results, especially in Upper General River catchment where high hazard and risk values were determined (Quesada-Román and Zamorano-Orozco, 2018, 2019a, 2019b).

At larger scales (i.e., at the state to district level), direct quantification of exposure is complex, and surveys must rely on proxy indicators (such as inhabitants or housing density) in many instances to give an estimated value of the exposure level (Allen et al., 2018). We obtained very realistic results for exposure using WorldPop (https://www.worldpop.org/) in the Térraba catchment when compared to available census data from 2011. As an open access, high-resolution source of information, these spatial demographic datasets were widely used in the past to support development and disaster response applications. For example, Phongsapan et al. (2019) used this database to determine a flood risk index at the national scale in Myanmar. The use of WorldPop for vulnerability determination in worldwide flood risk mapping assessments have been proved in the past (Tatem, 2017; Glas et al., 2019). Moreover, the use of social indexes such as the IDS 2017 (MIDEPLAN - Ministerio de Planificación Nacional y Política Económica, 2017) to determine the vulnerability shows the economic, social participation, health, educative, and security conditions of political-administrative units. Applying a social development index to calculate vulnerability also shows that other indexes (i.e., human development index at municipal scales) can be useful for risk assessments. For all the steps of analyses, however, it is important to consider the remaining uncertainties, resilience, and sensitivities of the social vulnerability indexes that are known to depend chiefly on outputs scale (Tate, 2012; Rufat et al., 2015; Spielman et al., 2020).

In the Térraba catchment, nearly 60% of the inhabitants live in rural settings and 40% of the workforce is associated with agriculture (INEC - Instituto Nacional de Estadística y Censos, 2020). Resilience in rural areas is driven primarily by community capital and there is considerable spatial variability in the components of disaster resilience (Cutter et al., 2016). Settlements closer to cities have more capacity to deal with floods (Jamshed et al., 2020) whereas rural areas in developing countries mostly remain disproportionately vulnerable to disasters. Their vulnerability to disaster often results in high migration rates, diffused benefit from social protection schemes, and scarce or non-existent savings to smooth the impacts (Deria et al., 2020). Furthermore, the Térraba catchment comprises several indigenous territories that should be assessed using the knowledge and cultural appropriation of risk management strategies by the indigenous population (Kelman et al., 2012). Consequently, rural and indigenous incomes depend on fewer livelihood assets, and they are more likely to live in vulnerable ecosystems (UNDRR – United Nations Disaster Risk Reduction, 2019). Therefore, the impact of disasters in the Térraba catchment will likely affect lower income households in rural settings the most (Jakobsen, 2012; Arouri et al., 2015). In this sense, policy instruments such as land-use management, poverty reduction, and environmental management can help manage disaster risks (Lavell and Maskrey, 2014).

During the first week of November 2020, Hurricane Eta (category 4) impacted Central America. Preliminary reports indicate economic losses that would exceed 5 US billion dollars. Hurricane Eta will be remembered as the worst tropical cyclone in decades in Central America, comparable to Hurricane Mitch in 1998. Indirect effects of tropical cyclones normally affect the Pacific slope of Costa Rica (Hidalgo et al., 2020), as what occurred during Eta in November 2020. Interestingly, one of the most affected regions by this event within Costa Rica was the Térraba catchment.

A preliminary qualitative cross validation of our results against the national authorities' field surveys (CNE – Comisión Nacional de Prevención de Riesgos y Atención de Emergencias, 2021) indicates that the sub-catchments in the mountain areas of the Térraba catchment for which we calculated the highest risk (i.e., the areas close to San Isidro, Buenos Aires, and San Vito) were also those who were affected heavily by the flooding from Hurricane Eta. Moreover, economic impacts were reported to be 87 US million dollars in all the municipalities integrating the catchment. The most affected economic sectors were streets (41%), bridges (32%), housing (15%), and river rehabilitation (8%; CNE – Comisión Nacional de Prevención de Riesgos y Atención de Emergencias, 2021).

Despite the legitimate scientific and technical production of flood studies in Costa Rica, regional high-resolution flood risk assessments in large-scale catchments, such as Térraba, are still critically missing (Quesada-Román et al., 2020d). The approach presented in this study proves critical for mountain tropical and low-latitude regions as the expected economic losses and social developments will make these

countries more vulnerable to tropical cyclones and floods (Shi and Karsperson, 2015). Many urban centers in tropical mountain regions are affected by uncontrolled growth or urban sprawl, which will favor disaster occurrence (Zhou et al., 2019). Therefore, an integration of risk management and climate change scenarios is critically needed in urban planning processes (Park and Lee, 2019; Pinos et al., 2020). Without a clear land-use planning and the enforcement of regulatory plans, disaster risk will continue to increase. In cases for which baseline information is lacking, innovative and practical approaches must be applied to assist disaster risk assessment effectively (Quesada-Román and Villalobos-Chacón, 2020).

5. Conclusions

We performed a regional flood-frequency analysis along with a risk assessment that includes hazard, exposure, and vulnerability mapping to address the impacts associated with floods triggered by tropical cyclones in the Térraba catchment, Costa Rica. We used a 10-y return period as a reliable time window for the recurrence of tropical cyclones and as it allows determination of the flood risk in a large catchment with observed and not extrapolated data. Peak discharges occurring after the passage of tropical cyclones were determined using flood-frequency and dendrogeomorphic records. The combination of approaches has proven suitable in the data-limited Térraba catchment where approximately 6000 inhabitants are located in flood-prone areas. Our results illustrate spatial variations of risk and coincide with the areas that have been hit by the floods triggered by Hurricane Eta in November 2020, causing millions of US dollars in economic impacts, mainly in streets, bridges, housing and the rehabilitation of rivers. This approach can thus be considered a useful input for land-use planning and disaster risk reduction, increasing the resilience of residents within the Térraba catchment in Costa Rica. Furthermore, this innovative and practical method may be successfully applied in developing and tropical countries for which hydrological data is often scarce or missing.

Declaration of competing interest

We the undersigned declare that this manuscript is original, has not been published before and is not currently being considered for publication elsewhere. We confirm that the manuscript has been read and approved by all named authors and that there are no other persons who satisfied the criteria for authorship but are not listed. We further confirm that the order of authors listed in the manuscript has been approved by all of us. We understand that the Corresponding Author is the sole contact for the Editorial process. He is responsible for communicating with the other authors about progress, submissions of revisions and final approval of proofs.

Acknowledgments

We greatly acknowledge to Berny Fallas and the Hydrology Area of the Basic Studies Services Center of the Costa Rican Electricity Institute for the peak discharge information of hydrological stations along the catchment. Special thanks to Soll Kracher for her accurate corrections of English grammar. This work is part of a PhD project of AQR, funded by the Swiss Federal Commission for Scholarships (ESKAS-Nr 2017.1072), Ministry of Science, Technology and Communications of Costa Rica (No MICITT-PINN-CON-2-1-4-17-1-002), and the University of Costa Rica (OAICE-187-2017). Finally, thanks to the anonymous reviewers and Scott A. Lecce for their valuable collaboration, suggestions and corrections that highly improved the manuscript.

Appendix A. Supplementary data

Supplementary data to this article can be found online at https://doi.org/10.1016/j.geomorph.2021.108000.

References

Acuña-Piedra, J.F., Quesada-Román, A., 2016. Evolución geomorfológica entre 1948 y 2012 del delta Térraba–Sierpe, Costa Rica. Cuat. Geomorfol. 30 (3-4), 49–73. https://doi.org/10.17735/cyg.v30i3-4.53055.

Acuña-Piedra, J.F., Quesada-Román, A., 2021. Multidecadal biogeomorphic dynamics of a deltaic mangrove forest in Costa Rica. Ocean Coast. Manag. 211, 105770.

Allen, S.K., Ballesteros-Cánovas, J.A., Randhawa, S.S., Singha, A.K., Huggel, C., Stoffel, M., 2018. Translating the concept of climate risk into an assessment framework to inform adaptation planning: Insights from a pilot study of flood risk in Himachal Pradesh, Northern India. Master Thesis in Environmental GeographyEnviron. Sci. Policy 87, 1–10.

Alvarado, L.F., Alfaro, E., 2003. Frecuencia de los ciclones tropicales que afectaron a Costa Rica durante el siglo XX. Tóp. Meteo. Ocean. 10 (1), 1–11.

Alvarado, G.E., Benito, B., Staller, A., Climent, A., Camacho, E., Rojas, W., Marroquín, G., Molina, E., Talavera, E., Martínez-Cuevas, S., Lindholm, C., 2017. The new central american seismic hazard zonation: Mutual consensus based on up to day seismotectonic framework. Tectonophysics 721, 462–476. https://doi.org/10.1016/j.tecto.2017.10.013.

Annis, A., Nardi, F., Morrison, R.R., Castelli, F., 2019. Investigating hydrogeomorphic floodplain mapping performance with varying DTM resolution and stream order. Hydrolog. Sci. J. 64 (5), 525–538.

Arcement, G.J., Schneider, V.R., 1989. Guide for selecting Manning's roughness coefficients for natural channels and flood plains. United States Geological Survey. Water-Supply Paper, p. 2339.

Arouri, M., Nguyen, C., Youssef, A.B., 2015. Natural disasters, household welfare, and resilience: evidence from rural Vietnam. World Dev. 70, 59–77. https://doi.org/10.1016/j.worlddev.2014.12.017.

Baker, V.R., 2008. Paleoflood hydrology: origin, progress, prospects. Geomorphology 101 (1), 1–13. https://doi.org/10.1016/j.geomorph.2008.05.016.

Ballesteros-Cánovas, J.A., Bodoque, J.M., Díez-Herrero, A., Sanchez-Silva, M., Stoffel, M., 2011a. Calibration of floodplain roughness and estimation of flood discharge based on tree-ring evidence and hydraulic modelling. J. Hydrol. 403, 103–115. https://doi.org/10.1016/j.jhydrol.2011.03.045.

Ballesteros-Cánovas, J.A., Eguibar, M., Bodoque, J.M., Díez-Herrero, A., Stoffel, M., Gutiérrez-Pérez, I., 2011b. Estimating flash flood discharge in an ungauged mountain catchment with 2D hydraulic models and dendrogeomorphic palaeostage indicators. Hydrol. Proc. 25, 970–979. https://doi.org/10.1002/hyp.7888.

Ballesteros-Cánovas, J.A., Sanchez-Silva, M., Bodoque, J.M., Díez-Herrero, A., 2013. An integrated approach to flood risk management: a case study of Navaluenga (Central Spain). Water Resour. Manag. 27 (8), 3051–3069.

Ballesteros-Cánovas, J.A., Stoffel, M., St George, S., Hirschboeck, K., 2015a. A review of flood records from tree rings. Prog. Phys. Geogr. 39 (6), 794–816. https://doi.org/10.1177/0309133315608758.

Ballesteros-Cánovas, J.A., Czajka, B., Janecka, K., Lempa, M., Kaczka, R.J., Stoffel, M., 2015b. Flash floods in the Tatra Mountain streams: frequency and triggers. Sci. Total Environ. 511, 639–648. https://doi.org/10.1016/j.scitotenv.2014.12.081.

Ballesteros-Cánovas, J.A., Stoffel, M., Spyt, B., Janecka, K., Kaczka, R.J., Lempa, M., 2016. Paleoflood discharge reconstruction in Tatra Mountain streams. Geomorphology 272, 92–101. https://doi.org/10.1016/j.geomorph.2015.12.004.

Ballesteros-Cánovas, J.A., Trappmann, D., Shekhar, M., Bhattacharyya, A., Stoffel, M., 2017. Regional flood-frequency reconstruction for Kullu district, Western Indian Himalayas. J. Hydrol. 546, 140–149. https://doi.org/10.1016/j.jhydrol.2016.12.059.

Ballesteros-Cánovas, J.A., Allen, S., Stoffel, M., 2019. The importance of robust baseline data on past flood events for regional risk assessment: a study case from Indian Himalayas. UNISDR Global Assessment Report.

Ballesteros-Cánovas, J.A., Koul, T., Bashir, A., del Pozo, J.M.B., Allen, S., Guillet, S., Rashid, I., Alamgir, S.H., Shah, M., Bhat, M.S., Alam, A., Stoffel, M., 2020a. Recent flood hazards in Kashmir put into context with millennium-long historical and tree-ring records. Sci. Total Environ. 722, 137875.

Ballesteros-Cánovas, J.A., Bombino, G., D'Agostino, D., Denisi, P., Labate, A., Stoffel, M., Zema, D.A., Zimbone, S.M., 2020b. Tree-ring based, regional-scale reconstruction of flash floods in Mediterranean mountain torrents. Catena 189, 104481.

Barnes, H.H., 1967. Roughness characteristics of natural channels. United States Geological Survey. Water-Supply Paper, p. 1849.

Benito, G., Brázdil, R., Herget, J., Machado, M.J., 2015. Quantitative historical hydrology in Europe. Hydrol. Earth Syst. Sci. 19, 3517–3539.

Bhatia, K.T., Vecchi, G.A., Knutson, T.R., Murakami, H., Kossin, J., Dixon, K.W., Whitlock, C.E., 2019. Recent increases in tropical cyclone intensification rates. Nat. Commun. 10 (1), 1–9.

Bodoque, J.M., Díez-Herrero, A., Eguibar, M.A., Benito, G., Ruiz-Villanueva, V., Ballesteros-Cánovas, J.A., 2015. Challenges in paleoflood hydrology applied to risk analysis in mountainous watersheds–a review. J. Hydrol. 529, 449–467.

Bodoque, J.M., Ballesteros-Cánovas, J.A., Stoffel, M., 2020. An application-oriented protocol for flood frequency analysis based on botanical evidence. J. Hydrol. 125242. https://doi.org/10.1016/j.jhydrol.2020.125242.

Borga, M., Gaume, E., Creutin, J.D., Marchi, L., 2008. Surveying flash floods: gauging the ungauged extremes. Hydrol. Process. 22 (18), 3883–3885. https://doi.org/10.1002/hyp.7111.

Brooks, G., George, St, 2015. Flooding, structural flood control measures, and recent geomorphic research along the Red River, Manitoba, Canada. Geomorphic Approaches to Integrated Floodplain Management of Lowland Fluvial Systems in North America and Europe. Springer, New York, pp. 87–117.

Camacho, M.E., Quesada-Román, A., Mata, R., Alvarado, A., 2020. Soil-geomorphology relationships of alluvial fans in Costa Rica. Geoderma Reg. 21, e00258. https://doi.org/10.1016/j.geodrs.2020.e00258.

Carabella, C., Buccolini, M., Galli, L., Miccadei, E., Paglia, G., Piacentini, T., 2020. Geomorphological analysis of drainage changes in the NE Apennines piedmont area: the case of the middle Tavo River bend (Abruzzo, Central Italy). J. Maps 16 (2), 222–235.
Cea, L., Bladé, E., Sanz-Ramos, M., Bermúdez Pita, M., Mateos-Alonso, Á., 2019. Iber Applications Basic Guide. https://doi.org/10.17979/spudc.9788497497176.
Chow, V., 1959. Open-channel Hydraulics. McGraw-Hill, New York, p. 680.
CNE – Comisión Nacional de Prevención de Riesgos y Atención de Emergencias, 2021. Plan de Emergencia, Situación provocada por los efectos del Huracán Eta. Decreto Ejecutivo de Emergencia N° 42705-MP. San José, Costa Rica.
Cutter, S.L., Ash, K.D., Emrich, C.T., 2016. Urban–rural differences in disaster resilience. Ann. Am. Assoc. Geogr. 106 (6), 1236–1252. https://doi.org/10.1080/24694452.2016.1194740.
De Groeve, T., Vernaccini, L., Polansek, K., 2014. Index for Risk Management - InfoRM. Report EUR 26528 EN. https://doi.org/10.2788/78658.
Denyer, P., Alvarado, G.E., 2007. Mapa geológico de Costa Rica. Escala 1:400 000. Librería Francesa, San José, Costa Rica.
Deria, A., Ghannad, P., Lee, Y.C., 2020. Evaluating implications of flood vulnerability factors with respect to income levels for building long-term disaster resilience of low-income communities. Int. J. Disaster Risk Reduct. 48, 101608.
de Ruiter, M.C., Couasnon, A., van den Homberg, M.J., Daniell, J.E., Gill, J.C., Ward, P.J., 2020. Why we can no longer ignore consecutive disasters. Earth's Future 8 (3), e2019EF001425.
Díez-Herrero, A., Garrote, J., 2020. Flood risk analysis and assessment, applications and uncertainties: a bibliometric review. Water 12, 2050. https://doi.org/10.3390/w12072050.
Dramis, F., Guida, D., Cestari, A., 2011. Nature and aims of geomorphological mapping. In: Smith, M., Paron, P., Griffiths, J.M. (Eds.), Geomorphological Mapping. Developments in Earth Surface Processes. Elsevier, pp. 39–73.
Durán-Quesada, A.M., Sorí, R., Ordoñez, P., Gimeno, L., 2020. Climate perspectives in the intra-Americas seas. Atmosphere 11 (9), 959.
Gaál, L., Szolgay, J., Kohnová, S., Hlavčová, K., Viglione, A., 2010. Inclusion of historical information in flood frequency analysis using a Bayesian MCMC technique: a case study for the power dam Orlík, Czech Republic. Contrib. Geophysi. Geodesy 40 (2), 121–147.
Gardner, T.W., Fisher, D.M., Morell, K.D., Cupper, M.L., 2013. Upper-plate deformation in response to flat slab subduction inboard of the aseismic Cocos Ridge, Osa Peninsula, Costa Rica. Lithosphere 5 (3), 247–264. https://doi.org/10.1130/L251.1.
Garrote, J., Gutiérrez-Pérez, I., Díez-Herrero, A., 2019. Can the quality of the potential flood risk maps be evaluated? A case study of the social risks of floods in Central Spain. Water 11 (6), 1284.
Gaume, E., Gaál, L., Viglione, A., Szolgay, J., Kohnová, S., Blöschl, G., 2010. Bayesian MCMC approach to regional flood frequency analyses involving extraordinary flood events at ungauged sites. J. Hydrol. 394 (1-2), 101–117.
Gaume, E., 2018. Flood frequency analysis: the Bayesian choice. WIREs Water 5 (4), e1290.
Glas, H., Rocabado, I., Huysentruyt, S., Maroy, E., Salazar Cortez, D., Coorevits, K., De Maeyer, P., Deruyter, G., 2019. Flood risk mapping worldwide: a flexible methodology and toolbox. Water 11 (11), 2371.
Granados-Bolaños, S., Quesada-Román, A., Alvarado, G.E., 2021. Low-cost UAV applications in dynamic tropical volcanic landforms. J. Volcanol. Geotherm. Res. 410, 107143.
Guerriero, L., Ruzza, G., Guadagno, F.M., Revellino, P., 2020. Flood hazard mapping incorporating multiple probability models. J. Hydrol. 587, 125020.
Hidalgo, H.G., Durán-Quesada, A.M., Amador, J.A., Alfaro, E.J., 2015. The Caribbean Low-Level Jet, the Inter-Tropical Convergence Zone and precipitation patterns in the Intra-Americas Sea: a proposed dynamical mechanism. Geogr. Ann., Ser. A 97, 41–59. https://doi.org/10.1111/geoa.12085.
Hidalgo, H.G., Alfaro, E.J., HernÃandez-Castro, F., Pérez-Briceño, P.M., 2020. Identification of tropical cyclones' critical positions associated with extreme precipitation events in Central America. Atmosphere 11 (10), 1123.
Hosking, J.R., Wallis, J.R., 1987. Parameter and quantile estimation for the generalized Pareto distribution. Technometrics 29 (3), 339–349.
Hosking, J.R.M., Wallis, J.R., 1997. Regional Frequency Analysis: An Approach Based on L-Moments. Cambridge University Press, Cambridge, p. 224.
ICE - Instituto Costarricense de Electricidad, 2019. Registro de Caudales. Medios Anuales. Centro de Servicio Estudios Básicos de Ingeniería, Ingeniería & Construcción. San José, Costa Rica.
IMN - Instituto Meteorológico Nacional, 2008. Atlas Climatológico Interactivo. Available on https://www.imn.ac.cr/atlas-climatologico.
INEC - Instituto Nacional de Estadística y Censos, 2020. National population projections for 2020 based on 2011 National Census. San José, Costa Rica. Available on https://www.inec.cr/poblacion/estimaciones-y-proyecciones-de-poblacion.
IPCC, 2014. In: Field, C.B., Baros, V., Dokken, D.J., Mach, K.J., Mastrandrea, M.D., Bilir, T.E., Chatterjee, M., Ebi, K.L., Estrada, Y.O., Genova, R.C. (Eds.), Climate Change 2014: Impacts, Adaptation, and Vulnerability. Part A: Global and Sectoral Aspects. Contribution of Working Group II to the Fifth Assessment Report of the Intergovernmental Panel on Climate Change. Cambridge University Press, Cambridge, UK and New York, USA, p. 1132.
Jakobsen, K.T., 2012. In the eye of the storm—the welfare impacts of a hurricane. World Dev. 40 (12), 2578–2589. https://doi.org/10.1016/j.worlddev.2012.05.013.
Jamshed, A., Birkmann, J., Rana, I.A., Feldmeyer, D., 2020. The effect of spatial proximity to cities on rural vulnerability against flooding: an indicator based approach. Ecol. Indic. 118, 106704.
Jiang, B., 2013. Head/tail breaks: a new classification scheme for data with a heavy-tailed distribution. Prof. Geogr. 65 (3), 482–494.
Kelman, I., Mercer, J., Gaillard, J.C., 2012. Indigenous knowledge and disaster risk reduction. Geography 97 (1), 12–21.
Krishnaswamy, J., Halpin, P.N., Richter, D.D., 2001a. Dynamics of sediment discharge in relation to land-use and hydro-climatology in a humid tropical watershed in Costa Rica. J. Hydrol. 253, 91–109. https://doi.org/10.1016/S0022-1694(01)00474-7.
Krishnaswamy, J., Richter, D.D., Halpin, P.N., Hofmockel, M.S., 2001b. Spatial patterns of suspended sediment yields in a humid tropical watershed in Costa Rica. Hydrol. Proc. 15 (12), 2237–2257. https://doi.org/10.1002/hyp.230.
Krishnaswamy, J., Kelkar, N., Birkel, C., 2018. Positive and neutral effects of forest cover on dry-season stream flow in Costa Rica identified from Bayesian regression models with informative prior distributions. Hydrol. Proc. 32 (24), 3604–3614. https://doi.org/10.1002/hyp.13288.
Langhammer, J., Vacková, T., 2018. Detection and mapping of the geomorphic effects of flooding using UAV photogrammetry. Pure Appl. Geophys. 175 (9), 3223–3245. https://doi.org/10.1007/s00024-018-1874-1.
LA RED, 2018. DesInventar – inventory system of the effects of disasters.Available at: Corporación OSSA, Cali, Colombia Accessed 15 july 2020. http://desinventar.org.
Lavell, A., Maskrey, A., 2014. The future of disaster risk management. Environ. Hazards 13 (4), 267–280. https://doi.org/10.1080/17477891.2014.935282.
Lawrence, D., Vandecar, K., 2015. Effects of tropical deforestation on climate and agriculture. Nat. Clim. Chang. 5 (1), 27–36.
Maldonado, T., Rutgersson, A., Alfaro, E., Amador, J., Claremar, B., 2016. Interannual variability of the midsummer drought in Central America and the connection with sea surface temperatures. Adv. Geosci. 42, 35–50. https://doi.org/10.5194/adgeo-42-35-2016.
Meko, D.M., Woodhouse, C.A., Morino, K., 2012. Dendrochronology and links to streamflow. J. Hydrol. 412, 200–209.
MIDEPLAN - Ministerio de Planificación Nacional y Política Económica, 2017. Índice de Desarrollo Social 2017. MIDEPLAN, San José, Costa Rica, p. 126.
Nardi, F., Grimaldi, S., Santini, M., Petroselli, A., Ubertini, L., 2008. Hydrogeomorphic properties of simulated drainage patterns using digital elevation models: the flat area issue. Hydrolog. Sci. J. 53 (6), 1176–1193. https://doi.org/10.1623/hysj.53.6.1176.
Nardi, F., Annis, A., Di Baldassarre, G., Vivoni, E.R., Grimaldi, S., 2019. GFPLAIN250m a global high-resolution dataset of earth's floodplains. Sci. Data 6, 180309.
Nguyen, C.C., Gaume, E., Payrastre, O., 2014. Regional flood frequency analyses involving extraordinary flood events at ungauged sites: further developments and validations. J. Hydrol. 508, 385–396.
Park, K., Lee, M.H., 2019. The development and application of the urban flood risk assessment model for reflecting upon urban planning elements. Water 11 (5), 920.
Phongsapan, K., Chishtie, F., Poortinga, A., Bhandari, B., Meechaiya, C., Kunlamai, T., San Aung, K., Saah, D., Anderson, E., Markert, K., Markert, A., Towashiraporn, P., 2019. Operational flood risk index mapping for disaster risk reduction using Earth Observations and cloud computing technologies: a case study on Myanmar. Front. Environ. Sci. 7, 191.
Piacentini, T., Carabella, C., Boccabella, F., Ferrante, S., Gregori, C., Mancinelli, V., Pacione, A., Pagliani, T., Miccadei, E., 2020. Geomorphology-based analysis of flood critical areas in small hilly catchments for civil protection purposes and early warning systems: the case of the Feltrino stream and the Lanciano Urban Area (Abruzzo, Central Italy). Water 12 (8), 2228.
Pinos, J., Orellana, D., Timbe, L., 2020. Assessment of microscale economic flood losses in urban and agricultural areas: case study of the Santa Bárbara River, Ecuador. Nat. Hazards 103, 2323–2337.
Pinto Santos, P., Reis, E., Pereira, S., Santos, M., 2019. A flood susceptibility model at the national scale based on multicriteria analysis. Sci. Total Environ. 667, 325–337.
Pinto Santos, P., Pereira, S., Zêzere, J.L., Tavares, A.O., Reis, E., Garcia, R.A., Oliveira, S.C., 2020. A comprehensive approach to understanding flood risk drivers at the municipal level. J. Environ. Manag. 260, 110127.
Pourali, S.H., Arrowsmith, C., Chrisman, N., Matkan, A.A., Mitchell, D., 2016. Topography wetness index application in flood-risk-based land use planning. Appl. Spat. Anal. Policy 9 (1), 39–54.
Quesada-Román, A., 2016. Master Thesis in Environmental GeographyPeligros geomorfológicos: inundaciones y procesos de ladera en la cuenca alta del río General (Pérez Zeledón), Costa Rica. Universidad Nacional Autónoma de México, pp. 157. https://repositorio.unam.mx/contenidos/83125.
Quesada-Román, A., 2017. Geomorfología Fluvial e Inundaciones en la Cuenca Alta del Río General, Costa Rica. Anu. Inst. Geocienc. 40 (2), 278–288. https://doi.org/10.11137/2017_2_278_288.
Quesada-Román, A., 2020. Deciphering Natural Hazard Histories Based on Tree-ring Analyses in Contrasting Tropical Ecosystems of Costa Rica. University of Geneva Doctoral dissertation.
Quesada-Román, A., 2021. Landslides and floods zonation using geomorphological analyses in a dynamic catchment of Costa Rica. Rev. Cart. 102, 125–138. https://doi.org/10.35424/rcarto.i102.901.
Quesada-Román, A., Zamorano-Orozco, J.J., 2018. Peligros Geomorfológicos en Costa Rica: Cuenca Alta del Río General. Anu. Inst. Geocienc. 41 (3), 239–251. https://doi.org/10.11137/2018_3_239_251.
Quesada-Román, A., Stoffel, M., Ballesteros-Cánovas, J.A., Zamorano-Orozco, J.J., 2019. Glacial geomorphology of the Chirripó National Park, Costa Rica. J. Maps 15 (2), 538–545. https://doi.org/10.1080/17445647.2019.1625822.
Quesada-Román, A., Zamorano-Orozco, J.J., 2019a. Geomorphology of the Upper General River Basin, Costa Rica. J. Maps 15 (2), 95–101. https://doi.org/10.1080/17445647.2018.1548384.
Quesada-Román, A., Zamorano-Orozco, J.J., 2019b. Zonificación de procesos de ladera e inundaciones a partir de un análisis morfométrico en la cuenca alta del río General, Costa Rica. Inv. Geogr. 99, e59843. https://doi.org/10.14350/rig.59843.
Quesada-Román, A., Ballesteros-Cánovas, J.A., Guillet, S., Madrigal-González, J., Stoffel, M., 2020a. Neotropical Hypericum irazuense shrubs reveal recent ENSO variability in

costa rican páramo. Dendrochronologia 61, 125704. https://doi.org/10.1016/j.dendro.2020.125704.
Quesada-Román, A., Ballesteros-Cánovas, J.A., Granados-Bolaños, S., Birkel, C., Stoffel, M., 2020b. Dendrogeomorphic reconstruction of floods in a dynamic tropical river. Geomorphology 359, 107133. https://doi.org/10.1016/j.geomorph.2020.107133.
Quesada-Román, A., Campos, N., Alcalá-Reygosa, J., Granados-Bolaños, S., 2020c. Equilibrium-line altitude and temperature reconstructions during the last Glacial Maximum in Chirripó National Park, Costa Rica. J. S. Am. Earth Sci. 100, 102576. https://doi.org/10.1016/j.jsames.2020.102576.
Quesada-Román, A., Campos, N., Granados-Bolaños, S., 2021. Tropical glacier reconstructions during the last Glacial Maximum in Costa Rica. Rev. Mex. Cienc. Geol. 38 (1), 55–64. https://doi.org/10.22201/cgeo.20072902e.2021.1.1600.
Quesada-Román, A., Villalobos-Portilla, E., Campos-Durán, D., 2020d. Hydrometeorological disasters in urban areas of Costa Rica, Central America. Environ. Hazards. https://doi.org/10.1080/17477891.2020.1791034.
Quesada-Román, A., Mata-Cambronero, E., 2020. The geomorphic landscape of the Barva volcano, Costa Rica. Phys. Geogr. https://doi.org/10.1080/02723646.2020.1759762.
Quesada-Román, A., Villalobos-Chacón, A., 2020. Flash flood impacts of Hurricane Otto and hydrometeorological risk mapping in Costa Rica. Geogr. Tidsskr. 120 (2), 142–155. https://doi.org/10.1080/00167223.2020.1822195.
Raymond, C., Horton, R.M., Zscheischler, J., Martius, O., AghaKouchak, A., Balch, J., Bowen, S.G., Camargo, S.J., Hess, J., Kornhuber, K., Oppenheimer, M., Ruane, A.C., Wahl, T., White, K., 2020. Understanding and managing connected extreme events. Nat. Clim. Chang. 10, 611–621.
Reis Jr., D.S., Stedinger, J.R., 2005. Bayesian MCMC flood frequency analysis with historical information. J. Hydrology 313 (1–2), 97–116.
Rodríguez-Morata, C., Ballesteros-Cánovas, J.A., Rohrer, M., Espinoza, J.C., Beniston, M., Stoffel, M., 2018. Linking atmospheric circulation patterns with hydro-geomorphic disasters in Peru. Int. J. Climatol. 38 (8), 3388–3404.
Rufat, S., Tate, E., Burton, C.G., Maroof, A.S., 2015. Social vulnerability to floods: review of case studies and implications for measurement. Int. J. Disaster Risk Reduc. 14, 470–486.
Ruiz-Villanueva, V., Díez-Herrero, A., Bodoque, J.M., Ballesteros-Cánovas, J.A., Stoffel, M., 2013. Characterisation of flash floods in small ungauged mountain basins of Central Spain using an integrated approach. Catena 110, 32–43.
Sánchez-Murillo, R., Durán-Quesada, A.M., Esquivel-Hernández, G., Rojas-Cantillano, D., Birkel, C., Welsh, K., Sánchez-Llull, M., Alonso-Hernández, C.M., Tetzlaff, D., Soulsby, C., Boll, J., Kurita, N., Cobb, K.M., 2019. Deciphering key processes controlling rainfall isotopic variability during extreme tropical cyclones. 10 (1), 1–10. https://doi.org/10.1038/s41467-019-12062-3.
Sánchez-Murillo, R., Esquivel-Hernández, G., Corrales-Salazar, J.L., Castro-Chacón, L., Durán-Quesada, A.M., Guerrero-Hernández, M., Delgado, V., Barberena, J., Montenegro-Rayo, K., Calderón, H., Chevez, C., Peña-Paz, T., García-Santos, S., Ortiz-Roque, P., Alvarado-Callejas, Y., Benegas, L., Hernández-Antonio, A., Matamoros-Ortega, M., Ortega, L., Terzer-Wassmuth, S., 2020. Tracer hydrology of the data-scarce and heterogeneous central American Isthmus. Hydrol. Process. 34 (11), 2660–2675.
Saunders, M.A., Lea, A.S., 2008. Large contribution of sea surface warming to recent increase in Atlantic hurricane activity. Nature 451, 557–560. https://doi.org/10.1038/nature06422.
Seybold, H., Berghuijs, W.R., Prancevic, J.P., Kirchner, J.W., 2021. Global dominance of tectonics over climate in shaping river longitudinal profiles. Nat. Geosci. 1–5.
Shi, P., Karsperson, R. (Eds.), 2015. World Atlas of Natural Disaster Risk. Springer, Heidelberg.
Sigafoos, R.S., 1964. Botanical evidence of floods and flood-plain deposition. Professional Paper, 485A. United States Geological Survey, p. 35.
Sörensen, R., Zinko, U., Seibert, J., 2006. On the calculation of the topographic wetness index: evaluation of different methods based on field observations. Hydrol. Earth Syst. Sci. 10, 101–112.
Spielman, S.E., Tuccillo, J., Folch, D.C., Schweikert, A., Davies, R., Wood, N., Tate, E., 2020. Evaluating social vulnerability indicators: criteria and their application to the Social Vulnerability Index. Nat. Hazards 100 (1), 417–436.
Stephens, T.A., Bledsoe, B.P., 2020. Probabilistic mapping of flood hazards: depicting uncertainty in streamflow, land use, and geomorphic adjustment. Anthropocene 29, 100231.
Stoffel, M., Casteller, A., Luckman, B.H., Villalba, R., 2012. Spatiotemporal analysis of channel wall erosion in ephemeral torrents using tree roots—an example from the Patagonian Andes. Geology 40 (3), 247–250.
St. George, S., Hefner, A.M., Avila, J., 2020. Paleofloods stage a come-back. Nat. Geosci. 13, 766–768. https://doi.org/10.1038/s41561-020-00664-2.
Syvitski, J.P., Cohen, S., Kettner, A.J., Brakenridge, G.R., 2014. How important and different are tropical rivers?—An overview. Geomorphology 227, 5–17.
Tate, E., 2012. Social vulnerability indices: a comparative assessment using uncertainty and sensitivity analysis. Nat. Hazards 63 (2), 325–347.
Tatem, A.J., 2017. WorldPop, open data for spatial demography. Sci. Data 4 (1), 1–4.
Tennille, S.A., Ellis, K.N., 2017. Spatial and temporal trends in the location of the lifetime maximum intensity of tropical cyclones. Atmosphere 8 (10), 198.
Turner, D., Lucieer, A., Watson, C., 2012. An automated technique for generating georectified mosaics from ultra-high resolution unmanned aerial vehicle (UAV) imagery, based on structure from motion (SfM) point clouds. Remote Sens. 4 (5), 1292–1410. https://doi.org/10.3390/rs4051392.
UNDRR – United Nations Disaster Risk Reduction, 2019. Global Assessment Report on Disaster Risk Reduction. United Nations Office for Disaster Risk Reduction (UNDRR), Geneva, Switzerland.
UNISDR, 2015. Sendai framework for disaster risk reduction 2015 - 2030. Third World Conference on Disaster Risk Reduction, Sendai, Japan, 14-18 March 2015 doi:A/CONF.224/CRP.1.
Veas-Ayala, N., Quesada-Román, A., Hidalgo, H., Alfaro, E., 2018. Humedales del Parque Nacional Chirripó, Costa Rica: características, relaciones geomorfológicas y escenarios de cambio climático. Rev. Biol. Trop. 66 (4), 1436–1448. https://doi.org/10.15517/rbt.v66i4.31477.
Vélez-Nicolás, M., García-López, S., Barbero, L., Ruiz-Ortiz, V., Sánchez-Bellón, Á., 2021. Applications of unmanned aerial systems (UASs) in hydrology: a review. Remote Sens. 13 (7), 1359.
Viglione, A., 2013. Non-supervised regional frequency analysis R library. http://cran.r-project.org/web/packages/nsRFA/.
Walsh, K.J., McBride, J.L., Klotzbach, P.J., Balachandran, S., Camargo, S.J., Holland, G., Knutson, T.R., Kossin, J.P., Tz.cheung, L., Sobel, A., Sugi, M., 2016. Tropical cyclones and climate change. Wiley Interdiscip. Rev. Clim. Chang. 7 (1), 65–89.
Webb, R.H., Jarrett, R.D., 2002. One-dimensional estimation techniques for discharges of paleofloods and historical floods. In: House, P.K., Webb, R.H., Baker, V.R., Levish, D.R. (Eds.), Ancient Floods, Modern Hazards: Principles and Applications of Paleoflood Hydrology: Water Science and Application. Vol. 5. American Geophysical Union, Washington, D.C, pp. 111–126.
Wilhelm, B., Ballesteros Cánovas, J.A., Macdonald, N., Toonen, W.H., Baker, V., Barriendos, M., Benito, G., Brauer, A., Corella, J.P., Denniston, R., Glaser, R., Ionita, M., Kahle, M., Liu, T., Luetscher, M., Macklin, M., Mudelsee, M., Munoz, S., Schulte, L., St. George, S., Stoffel, M., Wetter, O., 2019. Interpreting historical, botanical, and geological evidence to aid preparations for future floods. Wiley Interdiscip. Rev. Water 6 (1), e1318. https://doi.org/10.1002/wat2.1318.
Wohl, E., 2006. Human impacts to mountain streams. Geomorphology 79 (3-4), 217–248.
Wohl, E., Barros, A., Brunsell, N., Chappell, N.A., Coe, M., Giambelluca, T., ... Ogden, F., 2012. The hydrology of the humid tropics. Nat. Clim. Chang. 2 (9), 655–662.
Zhou, W., Jiao, M., Yu, W., Wang, J., 2019. Urban sprawl in a megaregion: a multiple spatial and temporal perspective. Ecol. Indic. 96, 54–66. https://doi.org/10.1016/j.ecolind.2017.10.035.